hypoxic ischaemia in rats (Hedtjarn *et al.* 2002; Jander *et al.* 2002). These data indicate a role for IL-18 in brain inflammatory responses, but the actions of IL-18 underlying this function, and its relationship to IL-1, have yet to be determined.

Microglia are the major source of IL-1β in the brain, particularly under inflammatory conditions (Hopkins and Rothwell 1995), and express IL-18 mRNA and protein constitutively *in vitro* (Conti *et al.* 1999; Prinz and Hanisch 1999). IL-18 and IL-1β are both expressed as inactive precursor molecules that lack a conventional signal peptide, are translated in the cytosol (Rubartelli *et al.* 1990; Okamura *et al.* 1995), cleaved by caspase-1 to the mature active peptides (Ghayur *et al.* 1997; Gu *et al.* 1997) and released by an unknown mechanism. Lipopolysaccharide (LPS) induces proIL-1β and proIL-18 expression in microglia (Conti *et al.* 1999), but is an inefficient stimulus for IL-1β secretion that requires a secondary stimulus. Extracellular adenosine triphosphate (ATP), the only endogenous secondary stimulus identified to date, can trigger efficient processing and release of IL-1β from LPS-primed monocytes and microglia, through activation of caspase-1 (Perregaux and Gabel 1994; Laliberte *et al.* 1999; Sanz and Di Virgilio 2000). We recently confirmed that ATP induced IL-1β release from microglia via the P2X7 receptor (Brough *et al.* 2002). ATP-induced secretion of IL-18 has been demonstrated in LPS-primed monocytes (Mehta *et al.* 2001).

The aims of this study were to test the hypothesis that IL-18 mimics the actions of IL-1β on murine glial cells, and to investigate the expression and release of IL-18 by microglia.

Materials and methods

Materials

Recombinant caspase-1 was a kind gift from Dr Nancy Thornberry (Merck Research Laboratory, Rahway, NJ, USA). Recombinant rat IL-1β, horseradish peroxidase (HRP)-conjugated anti-sheep IgG antibody and sheep anti-mouse IL-1β antibody were generously supplied by the National Institute of Biological Standards and Controls (NIBSC, Potters Bar, UK). Recombinant mouse IL-18 was purchased from R & D Biosystems (Minneapolis, MN, USA). Lipopolysaccharide (*Escherichia coli* serotype O55:B5) and ATP were purchased from Sigma-Aldrich Company Ltd, Gillingham, UK.

Animals

C57BL/6 mice in which the IL-18 or IL-1β gene had been deleted (Horai *et al.* 1998; Takeda *et al.* 1998) were used in this study. Mice were genotyped regularly to confirm knockout status. C57BL/6 mice (Charles River, Margate, UK) were used as controls. The animals were kept on a 12 : 12 h light–dark cycle at 21 ± 1°C, 45 ± 10% humidity with free access to food and water. All procedures were performed in accordance with UK legislation under the 1986 Animals (Scientific Procedures) Act.

Cell culture

Primary cultures of mixed glia were prepared using a modification of a previous protocol (McCarthy and de Vellis 1980). The brains of 0- to 3-day-old mouse pups were dissected, the meninges removed and the brain cells separated by passing through nylon membrane (80 μm) into medium. The pooled brain cells were seeded at 5×10^5 cells/mL and cultured in Dulbecco's modified Eagle's medium (DMEM; Invitrogen Ltd, Paisley, UK) supplemented with fetal bovine serum (10%; Invitrogen Ltd), penicillin (100 U/mL; Invitrogen Ltd) and streptomycin (100 μg/mL; Invitrogen Ltd), at 37°C, 5% CO_2 in a humidified atmosphere, until confluency [11–13 days *in vitro* (DIV)]. These cultures contained 10% Griffonia Simplicifolia lectin isolectin B4-positive microglia, 10% A2B5-positive O2A cells and 80% glial fibrillary acidic protein-positive astrocytes, as determined by immunocytochemistry. Secondary cultures of microglia were prepared by shaking confluent primary mixed glial cultures (15 *g*, 2 h, 37°C), using a heated shaking platform (New Brunswick Scientific Co., Inc., Hatfield, UK). The dislodged microglia were collected and seeded at 5×10^5 cells/mL. Weakly or non-adherent cells were removed by changing the medium after 1 h, and experiments were performed the following day. These cultures contained no astrocytes, as determined by immunocytochemistry.

RT–PCR

RNA was extracted from primary mixed glial or secondary microglial cell cultures using TRIzol reagent, according to the manufacturer's instructions (Invitrogen Ltd), and DNase-treated. cDNA was synthesized using murine myeloleukaemia virus reverse transcriptase (MMLV; Invitrogen Ltd), as described previously (Wheeler *et al.* 2000). PCR analysis was performed on cDNA equivalent to 0.15 μg total RNA in a total volume of 50 μL, containing forward and reverse primers (0.5 μM of each), PCR buffer (containing 1.5 mM $MgCl_2$; Qiagen, Crawley, UK), dNTP (200 μM) and Taq DNA polymerase (1.25 U; Qiagen). PCR was performed using a Hybaid Omn-E Thermocycler (Hybaid Ltd, Ashford, UK) with the following conditions: (i) 5 min at 95°C, 1 cycle; (ii) 30 s at 95°C, 30 s at 58°C, 45 s at 72°C, 40 cycles; (iii) 5 min at 72°C, 1 cycle. Specific primer sequences were used for murine IL-18Rβ, IL-18BP and GAPDH, as described previously (Wheeler *et al.* 2000), and for murine IL-18 (forward: CTTTGGAAGCCTGCTATAATCC, reverse: GGTCAAGAG-GAAGTGATTTGGA) and IL-18Rα (forward: TATAATTGCA-CCGTGGCCAAC, reverse: CGCCAGGCACCACATCTCTTT). PCR products were analysed on 2% agarose/TBE gels containing 0.4 μg/mL ethidium bromide. Controls included RT–PCR without cDNA, PCR using RNA as template, and PCR without cDNA or RNA. All yielded negative results, i.e. no detectable amplified products. The identity of the PCR products was confirmed by direct sequencing and comparison with published sequences. Two bands were detected for IL-18R and IL– 18BP; in each case, the upper one was specific whereas the lower one was a PCR artefact that showed no homology to published sequences.

Treatment of cells

Primary cultures of mixed glia or secondary cultures of microglia were incubated with vehicle [phosphate-buffered saline (PBS)], IL-18 (various doses), IL-1β (100 ng/mL) or LPS (1 μg/mL in mixed glia; 100 ng/mL in microglia) for 24 h. These doses of IL-1β

and LPS have been shown previously in our laboratory to induce robust responses in glial cells (Brough *et al.* 2002; Parker *et al.* 2002). Cell supernatants were then collected, and cell lysates prepared (see below). To investigate processing and release of IL-1β or IL-18, microglia were primed by incubation with vehicle (PBS), IL-18 (500 ng/mL) or LPS (100 ng/mL) for 24 h, and then treated for a further 3 h (unless otherwise stated) with ATP (5 mM). Cell supernatants were collected and cell lysates prepared (see below).

LDH assay

Cell death was determined by measuring lactate dehydrogenase (LDH) activity in the cell supernatants, using a commercial cytotoxicity assay (CytoTox 96 non-radioactive cytotoxicity assay; Promega, Madison, WI, USA), as described previously (Le Feuvre *et al.* 2002a).

Enzyme-linked immunosorbent assays

Cytokine content of glial cell lysates or supernatants was quantified using specific sandwich enzyme-linked immunosorbent assays (ELISAs). Mouse IL-18 ELISA was purchased from MBL Co. Ltd. (Nagoya, Japan), and used according to the manufacturer's instructions. ELISAs for murine IL-1α, IL-1β and IL-6 were generously supplied by Dr S. Poole (NIBSC; Le Feuvre *et al.* 2002a). Assay detection limits are stated for each result.

Western blot analysis

Cell lysates were prepared by lysing the cells on ice in 50 mM Tris (pH 7.5) containing β-glycerophosphate (50 mM), sodium orthovanadate (10 mM), sodium fluoride (5 mM), phenylmethylsulfonyl fluoride (1 mM) and Triton X-100 (1%). Protein content was determined using the Bio-Rad protein reagent (Bio-Rad Laboratories Ltd, Hemel Hempstead, UK). Proteins were resolved by sodium dodecyl sulphate polyacrylamide gel electrophoresis (SDS–PAGE) and transferred to nitrocellulose membrane. Non-specific binding was blocked by incubating the membrane in 10% low fat milk/0.02% Tween–PBS for 1 h at room temperature. The membranes were probed with goat anti-mouse IL-18 polyclonal antibody (1/500; Santa Cruz Biotechnology, Santa Cruz, CA, USA), sheep anti-mouse IL-1β antiserum (1/1000), or rabbit anti-actin (1/10000; Sigma-Aldrich Company Ltd) overnight at 4°C, followed by the appropriate HRP-conjugated secondary antibodies (1/4000; Autogen Bioclear UK Ltd, UK, except HRP–anti-sheep IgG; NIBSC) for 1 h at room temperature. Proteins were visualized by enhanced chemiluminescence (Amersham Pharmacia Biotech, Chalfont St. Giles, UK). Western blot results were quantified by densitometry (Northern Eclipse version 6.0; Empix Imaging Inc., North Tonawanda, New York, USA).

Statistical analysis

All results are expressed as mean ± SEM (n numbers are stated for each result) and analysed by one-way ANOVA with Tukey post-test unless otherwise stated. A probability (p) < 0.05 was considered significant.

Results

Expression of IL-18R complex on glial cells

To assess the ability of primary mixed glial and secondary microglial cell cultures to respond to IL-18, mRNA expression of IL-18Rα and IL-18Rβ was investigated by RT–PCR. Mixed glia and microglia expressed IL-18Rα and IL-18Rβ mRNAs, and also IL-18 and IL-18BP mRNAs constitutively, although IL-18Rα mRNA was present at very low levels (Fig. 1). All four molecules were expressed in liver, the positive control tissue.

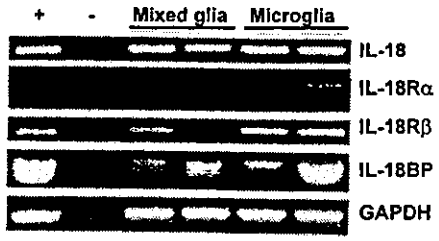

Fig. 1 Expression of IL-18, IL-18Rα, IL-18Rβ and IL-18BP mRNAs in murine primary mixed glial and secondary microglial cell cultures. RNA was extracted from confluent cultures, and cDNA was then synthesised and subjected to PCR (40 cycles) using specific primer pairs. The identity of these PCR products was confirmed by direct sequencing and comparison with published sequences. PCR product sizes were 216 bp for IL-18, 379 bp for IL-18Rα, 288 bp for IL-18Rβ, 370 bp for IL-18BP and 239 bp for GAPDH. Mouse liver was included as a positive control (+) and water (–) as a negative control. No genomic DNA was present, as assessed by PCR using RNA as template. Results from two independent cultures for each cell type are shown, representative of two PCR reactions.

Actions of IL-18 in mixed glial cells

The effect of IL-18 on cytokine expression and release was examined in primary mixed glial cell cultures. Treatment for 24 h with IL-18 induced a dose-dependent increase in intracellular proIL-1β (Fig. 2). However, no mature IL-1β was detected in the cell lysate by western blot (Fig. 2b). IL-18 (500 ng/mL) also induced intracellular expression of IL-1α and release of IL-6, but no IL-1β was detected in cell supernatants by ELISA (Fig. 3) or western blot (data not shown). In addition, IL-18 did not induce release of prostaglandin (PG)E2 or nitric oxide (data not shown). These responses were abolished by heat-treatment of IL-18 for 30 min at 95°C, indicating that the responses observed were not due to endotoxin contamination of the cytokine.

Effect of IL-18 on IL-1β expression and release in microglia

Treatment of microglia with IL-18 (500 ng/mL) for 24 h induced expression of proIL-1β, as assessed by western blot (Fig. 4a), to a level similar to that induced by LPS (100 ng/mL). Heat-treatment abolished this effect of IL-18. In addition, IL-18 had no effect on LDH release (data not shown).

As IL-18 stimulated proIL-1β expression similarly to LPS, we explored the possibility that IL-18 is a sufficient priming stimulus for ATP-induced processing and release of IL-1β.

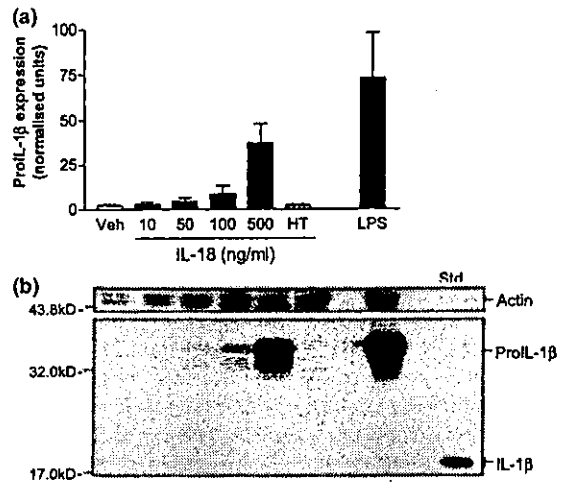

Fig. 2 Effect of IL-18 on proIL-1β expression in mixed glia. Confluent primary cultures of murine mixed glia were treated with PBS (Veh), IL-18 (10, 50, 100, or 500 ng/mL) or LPS (1 μg/mL) for 24 h. (a) Proteins in cell lysates (10 μg) were separated by SDS–PAGE and IL-1β and actin were detected by western blot. ProIL-1β expression was quantified by densitometry, expressed as a percentage of actin, and normalized to a standard (0.1 ng IL-1β) to allow comparison between blots. Results = mean ± SEM, $n = 4$. (b) A representative blot is shown (both bands for actin and proIL-1β were included in the analysis). No mature IL-1β was detected. HT, heat-treated IL-18 (500 ng/mL); Std, Recombinant mouse IL-1β (0.1 ng).

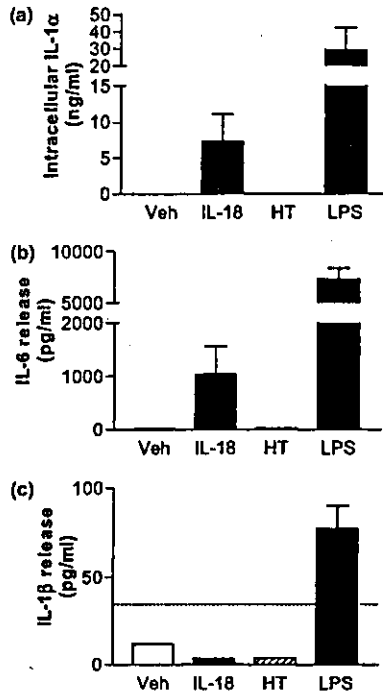

Fig. 3 Effect of IL-18 on cytokine expression and release in mixed glia. Confluent primary cultures of murine mixed glia were treated with PBS (Veh), IL-18 (500 ng/mL) or LPS (1 μg/mL) for 24 h. Intracellular IL-1α expression (a), and IL-6 (b) or IL-1β (c) release into the supernatant was measured by ELISA. Results shown are mean ± SEM, $n = 4$. Detection limit (dotted line) = 195 pg/mL (a), 15.6 pg/mL (b), 31.25 pg/mL (c). HT, heat-treated IL-18 (500 ng/mL).

Western blot analysis of cell supernatants was used to assess IL-1β release, as the available immunoassays did not distinguish between the precursor and mature forms. Cells primed with IL-18 (500 ng/mL) or LPS (100 ng/mL) for 24 h did not release any detectable IL-1β, but subsequent treatment with ATP for 3 h stimulated release of both precursor and mature forms of IL-1β (Fig. 4b). ATP did not affect IL-1β expression or release in unprimed microglia.

To investigate the involvement of endogenous IL-18 in IL-1β expression and release in response to LPS and ATP, microglial cultures were prepared from IL-18 knockout mice. Priming with LPS increased intracellular proIL-1β expression (Fig. 5A), and subsequent treatment with ATP induced significant release of IL-1β (Fig. 5B). However, there was no significant difference in IL-1β expression or release between wild-type and IL-18 knockout microglia under any of the conditions tested, nor was there any difference in basal proIL-1β expression (data not shown). Furthermore, there was no significant difference between wild-type and IL-18 knockout microglia in the proportion of precursor and mature IL-1β released after ATP treatment of LPS-primed cells, as assessed by quantification of western blots using densitometry (wild-type: 67.8 ± 5.2% proIL-1β and 41.2 ± 2.7% mature IL-1β; IL-18 knockout: 66.9 ± 3.8% proIL-1β and 36.9 ± 6.3% mature IL-1β). Wild-type and IL-18 knockout microglia did not differ significantly in LDH release in response to LPS and ATP (data not shown).

IL-18 expression and release in microglia

The effect of ATP on IL-18 release from LPS-primed microglia was investigated. No IL-18 was detected in cell supernatants by western blot, so IL-18 release was quantified using a commercial ELISA. IL-18 release was not detectable from untreated cells, cells primed with LPS alone, or unprimed cells treated with ATP. Release of IL-18 was detected 15 min after ATP treatment of LPS-primed microglia, and reached levels significantly different from vehicle after 3 h (1288 ± 493 pg/mL, $p < 0.05$; Fig. 6a). It was important to determine the affinity of the commercial ELISA for precursor and mature IL-18. Mouse brain homogenate contained only proIL-18, as assessed by western blot, and this was completely cleaved to the mature form by treatment with caspase-1 (Fig. 6bi). However, the IL-18 content was markedly greater in the caspase-1 treated sample than the PBS-treated sample when measured by ELISA (Fig. 6bii), indicating that the IL-18 ELISA had much higher affinity for mature IL-18 than proIL-18.

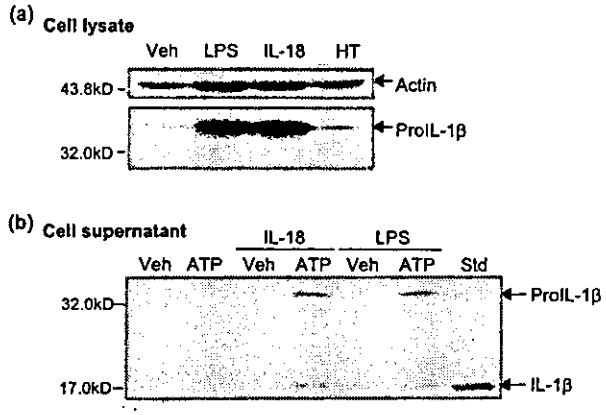

Fig. 4 Effect of IL-18 on IL-1β expression in microglia. (a) Intracellular IL-1β expression. Confluent secondary cultures of murine microglia were treated for 24 h with PBS (Veh), IL-18 (500 ng/mL), or LPS (100 ng/mL). Proteins in cell lysates (10 μg) were separated by SDS–PAGE and IL-1β and actin were detected by western blot. No mature IL-1β was detected. Representative of four independent experiments, performed in separate cultures. (b) Release of IL-1β. Confluent secondary microglial cultures were incubated for 24 h with PBS, IL-18 (500 ng/mL), or LPS (100 ng/mL), then treated for 3 h with PBS (Veh) or ATP (5 mM). Proteins in cell supernatants (10 μL) were separated by SDS–PAGE and IL-1β was detected by western blot. Representative of two independent experiments, performed in separate cultures. HT, heat-treated IL-18 (500 ng/mL); Std, recombinant mouse IL-1β (0.1 ng).

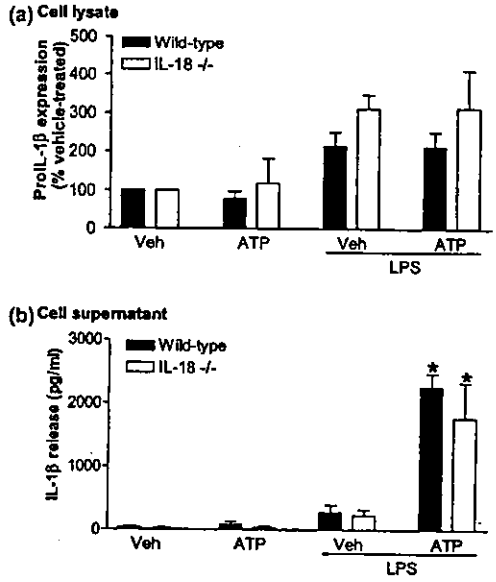

Fig. 5 IL-1β expression and secretion in wild-type (■) and IL-18 (□) knockout microglia. Secondary cultures of microglia were prepared from C57BL/6 (wild-type) or IL-18 knockout (IL-18 –/–) mice. Confluent cultures were incubated with PBS or LPS (100 ng/mL) for 24 h and then treated with PBS (Veh) or ATP (5 mM) for 3 h. (a) Proteins in cell lysates (10 μg) were separated by SDS–PAGE and IL-1β and actin were detected by western blot. Intracellular proIL-1β expression was quantified by densitometry, normalized to actin expression, and expressed as a percentage of expression in vehicle-treated cells. Results are mean ± SEM, $n = 3$. There were no significant differences in proIL-1β expression in wild-type and IL-18 knockout cultures, using one-way ANOVA with post-test analysis. (b) Release of IL-1β into the supernatant was quantified using an ELISA with equal affinity for precursor and mature IL-1β (Le Feuvre *et al.* 2002a). Results are mean ± SEM, $n = 4$. Results were analysed by one-way ANOVA with post-test analysis. $^*p < 0.001$ compared with vehicle-treated samples. Detection limit = 7.8 pg/mL.

Effect of IL-1β on IL-18 expression and release in microglia

As IL-18 induced proIL-1β expression in microglia, we investigated whether IL-1β exerted reciprocal actions on IL-18 expression. Treatment of microglia with IL-1β (100 ng/mL) for 24 h did not upregulate proIL-18 expression, although these cells were responsive to LPS (Fig. 7).

To investigate the involvement of endogenous IL-1β in IL-18 expression and release, microglial cultures were prepared from IL-1β knockout mice. As shown in Fig. 8(a), priming with LPS upregulated proIL-18 expression, and this was reduced by subsequent treatment with ATP. There was no significant difference in intracellular proIL-18 expression between wild-type and IL-1β knockout microglia in response to LPS and ATP. Release of IL-18 was detected only after ATP treatment of LPS-primed microglia, and was significantly reduced in IL-1β knockout microglia compared to wild-type microglia (224 ± 55 pg/mL and 806 ± 149 pg/mL, respectively, $p < 0.01$; Fig. 8b).

Discussion

We have demonstrated here that IL-18 induces intracellular expression of IL-1α and proIL-1β, as well as release of IL-6 from murine primary mixed glial cultures. In secondary microglial cultures, IL-18 induced proIL-1β expression, and subsequent treatment with ATP induced secretion of mature IL-1β. These observations suggest mechanisms by which IL-18 may be involved in inflammatory processes in the brain. LPS is a potent stimulus of intracellular proIL-1β expression in microglia, but our data suggest that this effect is not mediated by IL-18, as LPS-induced expression of proIL-1β, and secretion of IL-1β after subsequent treatment with ATP, was not altered in IL-18 knockout microglia. Expression of proIL-18 was induced by LPS, and subsequent treatment with ATP stimulated cellular release of IL-18. IL-1β did not induce proIL-18 expression in microglia, and LPS-induced proIL-18 expression was not altered in IL-1β knockout microglia. However, ATP-induced release of IL-18 from LPS-primed microglia was significantly reduced in IL-1β knockout mice, suggesting that IL-1β is involved in the processing and/or secretion of IL-18.

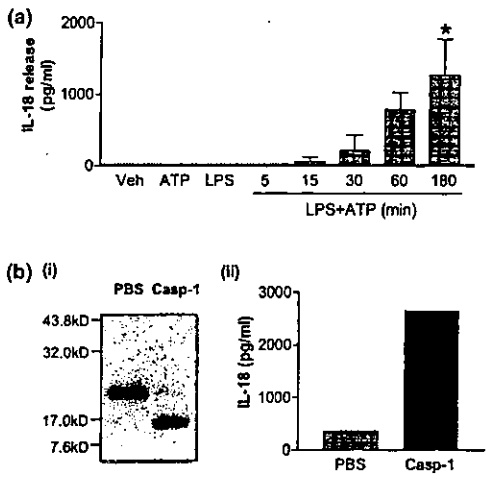

Fig. 6 ATP-induced release of IL-18 from LPS-primed microglia. (a) Confluent secondary cultures of murine microglia were incubated for 24 h with PBS or LPS (100 ng/mL), then treated with PBS (Veh) for 3 h, or ATP (5 mM) for 3 h (vehicle-primed cells) or a variable length of time (LPS-primed cells). IL-18 release into the supernatant was quantified using a commercial IL-18 ELISA. Results were analysed by one-way ANOVA with post-test analysis. Results = mean ± SEM, $n = 3$. $^*p < 0.05$ compared with vehicle-treated samples. Detection limit (dotted line) = 25 pg/mL. (b) Mouse brain homogenate (40 μg) was incubated with PBS or caspase-1 (Casp-1, 100 U) in 10 mM dithiothreitol (DTT) for 1 h at 37°C. IL-18 content was then assessed by western blot (bi) or commercial ELISA (bii). Only proIL-18 was present in brain homogenate, and this was completely cleaved to the mature form by caspase-1 treatment. The commercial ELISA detected greater levels of IL-18 in caspase-1-treated brain homogenate than PBS-treated, indicating greater affinity for mature IL-18.

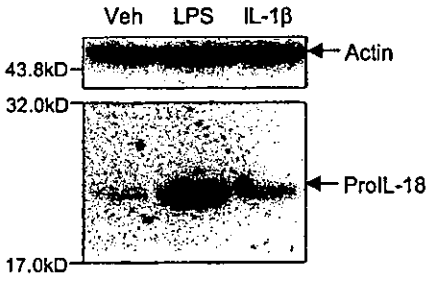

Fig. 7 Effect of IL-1β on IL-18 expression in microglia. Confluent secondary cultures of murine microglia were treated for 24 h with PBS (Veh), LPS (100 ng/mL), or IL-1β (100 ng/mL). Proteins in cell lysates (20 μg) were separated by SDS–PAGE. IL-18 and actin were detected by western blot. Representative of two independent experiments, performed in separate cultures. IL-1β did not upregulate proIL-18 expression, as determined by quantification of western blots by densitometry.

IL-18 actions in glia

Primary mixed glial and secondary microglial cultures constitutively expressed mRNAs encoding the two chains of the IL-18 receptor complex, IL-18Rα and IL-18Rβ,

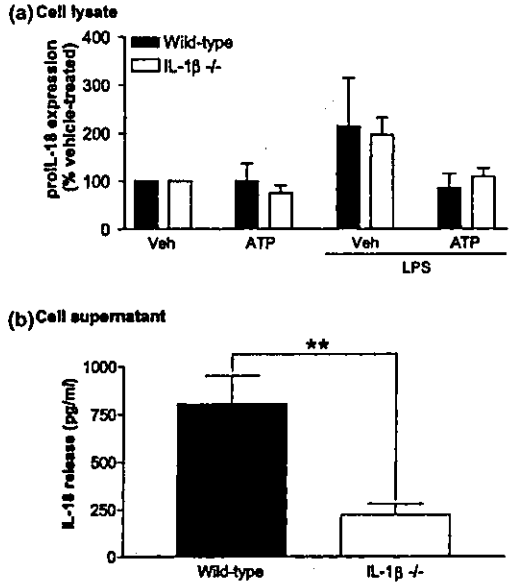

Fig. 8 IL-18 expression and secretion in wild-type (■) and IL-1β (□) knockout microglia. Secondary cultures of microglia were prepared from C57BL/6 (wild-type) or IL-1β knockout (IL-1β –/–) mice. Confluent cultures were incubated with PBS or LPS (100 ng/mL) for 24 h and then treated with PBS (Veh) or ATP (5 mM) for 3 h. (a) Proteins in cell lysates (20 μg) were separated by SDS–PAGE and IL-18 and actin were detected by western blot. Intracellular proIL-18 expression was quantified by densitometry, normalized to actin expression, and expressed as a percentage of expression in vehicle-treated cells. Results are mean ± SEM, $n = 4$ (wild-type), $n = 6$ (IL-1β –/–). There were no significant differences in proIL-1β expression between wild-type and IL-1β knockout cultures, using one-way ANOVA with post-test analysis. (b) IL-18 release into the supernatant was quantified by ELISA. IL-18 release was detected only after ATP treatment of LPS-primed microglia. Results are mean ± SEM, $n = 7$ (wild-type), $n = 6$ (IL-1β –/–). Results were analysed by one-way ANOVA with post-test analysis. $^{**}p < 0.01$. Detection limit (dotted line) = 10 pg/mL.

suggesting that these cells were potentially capable of responding to IL-18. Consistent with this, IL-18 induces recruitment of TRAF6 by IRAK in mouse microglia (Prinz and Hanisch 1999). IL-18 and IL-18BP mRNAs were also expressed constitutively. We investigated the effect of IL-18 on mediators known to be induced by IL-1β, i.e. PGE2, IL-6 and nitric oxide (Molina-Holgado *et al.* 2000), and demonstrate here for the first time that IL-18 induces release of IL-6 and intracellular expression of IL-1α and proIL-1β in murine-mixed glial cells. Heat-treatment abolished these responses, indicating that endotoxin contamination of the cytokine was not responsible for these effects. However, IL-18 did not induce release of nitric oxide or PGE2. Similarly, IL-18 induces expression of IL-1β mRNA and proIL-1β in human peripheral blood mononuclear cells, and fails to induce release of PGE2 (Puren *et al.* 1998; Reznikov *et al.* 2000).

Two receptor affinities have been reported for the IL-18 receptor complex: 0.4 nM and 11 nM (Debets *et al.* 2000). Thus, the highest dose used (500 ng/mL or 28 nM) should be sufficient to induce a maximal response, though this is a higher dose than is commonly used for cytokines *in vitro*. IL-18 was not toxic to the cells at any dose, as assessed by measuring LDH release, consistent with previous reports (Prinz and Hanisch 1999). It is possible that glial cells constitutively secrete IL-18BP, a potent inhibitor of IL-18, and that the high dose is required to overcome this inhibition. Consistent with this, IL-18BP mRNA was expressed constitutively at high levels in mixed glial and microglial cell cultures (Fig. 1). To date, there have been no studies reporting extracellular levels of IL-18BP protein in such cultures.

LPS induces expression of proIL-1β, but is an inefficient stimulus for IL-1β processing and secretion that requires a secondary stimulus, such as ATP, although ATP alone cannot induce IL-1β secretion (Perregaux and Gabel 1994). Microglia from IL-18 knockout and wild-type mice showed comparable IL-1β expression and processing in response to LPS and ATP. We have obtained similar results in macrophages (Le Feuvre *et al.* 2002a). This suggests that although IL-18 induced proIL-1β expression, it did not mediate the induction of proIL-1β by LPS, nor was it involved in IL-1β release, as induced by ATP. However, we demonstrate here that IL-18 could substitute for LPS as a priming stimulus for ATP-induced release of IL-1β. This may be particularly relevant to IL-1β secretion in pathophysiological conditions that are not associated with severe infection. For instance, in diseases associated with peripheral immune cell infiltration of the brain, such as multiple sclerosis or stroke, activated macrophages could release IL-18, priming resident microglia to respond to ATP by releasing mature IL-1β. ATP is released by activated immune cells and dying cells, and extracellular ATP concentrations are elevated under inflammatory conditions and in response to tissue trauma (for review, see Le Feuvre *et al.* 2002b). The mechanisms underlying the priming required for ATP-induced IL-1β secretion have not been clearly defined, but their elucidation may shed light on this action of IL-18.

Expression and release of IL-18 from microglia

In the experimental paradigm used in these studies, LPS induced expression of proIL-1β and proIL-18 in murine microglia, and subsequent treatment with ATP induced processing and release of mature IL-1β, as reported previously (Conti *et al.* 1999; Sanz and Di Virgilio 2000). In addition, we demonstrate that ATP induced release of IL-18 from LPS-primed microglia, consistent with previous studies in monocytes (Mehta *et al.* 2001).

IL-1β did not affect IL-18 expression by microglia. Consistent with this, LPS-induced expression of proIL-18 was not altered in IL-1β knockout microglia. More extensive studies in our lab suggest that microglia do not respond to exogenous IL-1β (Pinteaux *et al.* 2002), implying that the actions of IL-1β may be cell specific in the brain, perhaps determined by receptor expression.

However, IL-18 release in response to ATP was reduced markedly in LPS-primed IL-1β knockout microglia (Fig. 8), despite intracellular proIL-18 levels being comparable to wild-type microglia. This suggests a change in the processing or release mechanism. We have reported recently that ATP induces release of IL-1α from LPS-primed wild-type but not IL-1β knockout microglia (Brough *et al.* 2002). This reduction in release of IL-18 and IL-1α is not due to differences in ATP-induced cell death, as wild-type and IL-1β knockout microglia show no difference in LDH release in response to LPS and ATP (Brough *et al.* 2002). The decrease in supernatant IL-18 content may represent a reduction in total IL-18 released, indicating a role for IL-1β in the release mechanism. However, this would suggest that there is enhanced degradation of IL-18 protein in IL-1β knockout microglia, e.g. by caspase-3 (Akita *et al.* 1997), otherwise an increase in intracellular IL-18 would be observed relative to wild-type microglia. Alternatively, this result may represent a decrease in the proportion of mature IL-18 released, as the ELISA used has a much higher affinity for mature IL-18 than proIL-18 (Fig. 6b), therefore suggesting a role for IL-1β in efficient cleavage of IL-18 by caspase-1. IL-18 could not be detected in cell supernatants by western blot under any of the conditions tested in this study, presumably due to insufficient sensitivity, but a more sensitive technique such as immunoprecipitation could be used to clarify these results by determining the proportion of precursor and mature IL-18.

Interactions between IL-1β and IL-18

We, and others, have hypothesized that proIL-18 and proIL-1β compete for cleavage by caspase-1 (Akita *et al.* 1997; Culhane *et al.* 1998). The data presented here are not consistent with this hypothesis, but instead suggest that endogenous IL-1β is required for efficient processing and/or release of IL-18. Microglia *in vitro* appear to be unresponsive to exogenous IL-1β (as discussed above), suggesting that IL-1β acts intracellularly, rather than in an autocrine manner *via* membrane receptors. Thus IL-1β, or perhaps the pro-domain of IL-1β, could be required for some step in the processing pathway, e.g. recruitment of caspase-1 or other required proteins to secretory vesicles, or regulation of vesicle movement (Andrei *et al.* 1999). However, these are only speculations because to date, the mechanisms by which IL-1β and IL-18 are processed and released are very poorly understood. Despite the ability of IL-18 to induce proIL-1β expression, we found no evidence for IL-18 being required for IL-1β processing, suggesting that IL-18 and IL-1β do not exert reciprocal actions in their processing pathway.

IL-1β and IL-18 share several properties, including protein folding, synthesis as inactive precursors that lack a signal

peptide, and activation by caspase-1, and act via related receptor complexes to induce similar signalling pathways (Fantuzzi and Dinarello 1999; Fitzgerald and O'Neill 2000). Despite their similarities, these two cytokines exhibit considerable differences in their expression, regulation and actions. IL-1β is present only at very low levels in normal brain tissue, whereas IL-18 is expressed constitutively at high levels in the brain (Culhane *et al.* 1998). IL-1β is upregulated within 4 h of focal ischaemia, consistent with the ability of IL-1 receptor antagonist to reduce ischaemic damage, but IL-18 is upregulated much later, at time points associated with infiltration of peripheral immune cells (Jander *et al.* 2002). The data reported here reveal complex interactions between these two cytokines, as well as demonstrating further differences in their actions. Clarification of the mechanisms underlying the processing pathway of IL-1β and IL-18 is required in order to understand how these proinflammatory cytokines are regulated, and may be of particular significance for the design of pharmacological interventions to treat diseases in which these two cytokines play a prominent role, such as multiple sclerosis and stroke.

Acknowledgements

This work was supported in part by the Biotechnology and Biological Sciences Research Council, UK (RDW and DB) and the Medical Research Council, UK (NJR). ELISA reagents were generously supplied by the NIBSC, and recombinant caspase-1 by Dr Nancy Thornberry (Merck Research Laboratory, New Jersey, USA). The authors would like to thank Dr R. Gibson and Dr E. Pinteaux for their help in preparing this manuscript.

References

Akita K., Ohtsuki T., Nukada Y., Tanimoto T., Namba M., Okura T., Takakura Yamamoto R., Torigoe K., Gu Y., Su M. S. S., Fujii M., Satoh Itoh M., Yamamoto K., Kohno K., Ikeda M. and Kurimoto M. (1997) Involvement of caspase-1 and caspase-3 in the production and processing of mature human interleukin-18 in monocytic THP.1 cells. *J. Biol. Chem.* **272**, 26595–26603.

Allan S. M. and Rothwell N. J. (2001) Cytokines and acute neurodegeneration. *Nat. Rev. Neurosci.* **2**, 734–744.

Andrei C., Dazzi C., Lotti L., Torrisi M. R., Chimini G. and Rubartelli A. (1999) The secretory route of the leaderless protein interleukin 1β involves exocytosis of endolysosome-related vesicles. *Mol. Biol. Cell* **10**, 1463–1475.

Bazan J. F., Timans J. C. and Kastelein R. A. (1996) A newly defined interleukin-1? *Nature* **379**, 591.

Brough D., Le Feuvre R. A., Iwakura Y. and Rothwell N. J. (2002) Purinergic (P2X7) Receptor activation of microglia induces cell death via an interleukin-1-independent mechanism. *Mol. Cell. Neurosci.* **19**, 272–280.

Conti B., Park L. C., Calingasan N. Y., Kim Y., Kim H., Bae Y., Gibson E. and Joh T. H. (1999) Cultures of astrocytes and microglia express interleukin 18. *Brain Res. Mol. Brain Res.* **67**, 46–52.

Culhane A. C., Hall M. D., Rothwell N. J. and Luheshi G. N. (1998) Cloning of rat brain interleukin-18 cDNA. *Mol. Psychiatry* **3**, 362–366.

Debets R., Timans J. C., Churakowa T., Zurawski S., de Waal Malefyt R., Moore K. W., Abrams J. S., O'Garra A., Bazan J. F. and Kastelein R. A. (2000) IL-18 Receptors, their role in ligand binding and function: anti-IL-1RAcPL antibody, a potent antagonist of IL-18. *J. Immunol.* **165**, 4950–4956.

Fantuzzi G. and Dinarello C. A. (1999) Interleukin-18 and interleukin-1β: two cytokine substrates for ICE (caspase-1). *J. Clin. Immunol.* **19**, 1–11.

Fassbender K., Mielke O., Bertsch T., Muehlhauser F., Hennerici M., Kurimoto M. and Rossol S. (1999) Interferon-γ-inducing factor (IL-18) and interferon-γ in inflammatory CNS diseases. *Neurology* **53**, 1104–1106.

Fitzgerald K. A. and O'Neill L. A. (2000) The role of the interleukin-1/Toll-like receptor superfamily in inflammation and host defence. *Microbes Infect.* **2**, 933–943.

Gatti S., Beck J., Fantuzzi G., Bartfai T. and Dinarello C. A. (2002) Effect of interleukin-18 on mouse core body temperature. *Am. J. Physiol. Regul. Integr. Comp. Physiol.* **282**, R702–R709.

Ghayur T., Banerjee S., Hugunin M., Butler D., Herzog L., Carter A., Quintal L., Sekut L., Talanian R., Paskind M., Wong W., Kamen R., Tracey D. and Allen H. (1997) Caspase-1 processes IFN-γ-inducing factor and regulates LPS-induced IFN-γ production. *Nature* **386**, 619–623.

Gu Y., Kuida K., Tsutsui H., Ku G., Hsiao K., Fleming M. A., Hayashi N., Higashino K., Okamura H., Nakanishi K., Kurimoto M., Tanimoto T., Flavell R. A., Sato V., Harding M. W., Livingston D. J. and Su M. S. S. (1997) Activation of interferon-τ inducing factor mediated by interleukin-1β converting enzyme. *Science* **275**, 206–209.

Hedtjarn M., Leverin A. L., Eriksson K., Blomgren K., Mallard C. and Hagberg H. (2002) Interleukin-18 involvement in hypoxic-ischemic brain injury. *J. Neurosci.* **22**, 5910–5919.

Hopkins S. J. and Rothwell N. J. (1995) Cytokines and the nervous system. I: Expression and recognition. *Trends Neurosci.* **18**, 83–88.

Horai R., Asano M., Sudo K., Kanuka H., Suzuki M., Nishihara M., Takahashi M. and Iwakura Y. (1998) Production of mice deficient in genes for interleukin (IL)-1α, IL-1β, IL-1α/β, and IL-1 receptor antagonist shows that IL-1β is crucial in turpentine-induced fever development and glucocorticoid secretion. *J. Exp. Med.* **187**, 1463–1475.

Jander S. and Stoll G. (1998) Differential induction of interleukin-12, interleukin-18, and interleukin-1β converting enzyme mRNA in experimental autoimmune encephalomyelitis of the Lewis rat. *J. Neuroimmunol.* **91**, 93–99.

Jander S. and Stoll G. (2001) Interleukin-18 is induced in acute inflammatory demyelinating polyneuropathy. *J. Neuroimmunol.* **114**, 253–258.

Jander S., Schroeter M. and Stoll G. (2002) Interleukin-18 expression after focal ischemia of the rat brain: association with the late-stage inflammatory response. *J. Cereb. Blood Flow Metab.* **22**, 62–70.

Kubota T., Fang J., Brown R. A. and Krueger J. M. (2001) Interleukin-18 promotes sleep in rabbits and rats. *Am. J. Physiol. Regul. Integr. Comp. Physiol.* **281**, R828–R838.

Laliberte R. E., Eggler J. and Gabel C. A. (1999) ATP treatment of human monocytes promotes caspase-1 maturation and externalization. *J. Biol. Chem.* **274**, 36944–36951.

Le Feuvre R. A., Brough D., Iwakura Y., Takeda T. and Rothwell N. J. (2002a) Priming of macrophages with lipopolysaccharide potentiates P2X7-mediated cell death via a caspase-1-dependent mechanism, independently of cytokine production. *J. Biol. Chem.* **277**, 3210–3218.

Le Feuvre R. A., Brough D. and Rothwell N. J. (2002b) Extracellular ATP and P2X7 receptors in neurodegeneration. *Eur. J. Pharmacol.* **447**, 261–269.

McCarthy K. D. and de Vellis J. (1980) Preparation of separate astroglial and oligodendroglial cell cultures from rat cerebral tissue. *J. Cell Biol.* **85**, 890–902.

Mehta V. B., Hart J. and Wewers M. D. (2001) ATP-stimulated release of interleukin (IL)-1beta and IL-18 requires priming by lipopolysaccharide and is independent of caspase-1 cleavage. *J. Biol. Chem.* **276**, 3820–3826.

Molina-Holgado F., Toulmond S. and Rothwell N. J. (2000) Involvement of interleukin-1 in glial responses to lipopolysaccharide: endogenous versus exogenous interleukin-1 actions. *J. Neuroimmunol.* **111**, 1–9.

Nakanishi K., Yoshimoto T., Tsutsui H. and Okamura H. (2001) Interleukin-18 regulates both Th1 and Th2 responses. *Annu. Rev. Immunol.* **19**, 423–474.

Okamura H., Tsutsi H., Komatsu T., Yutsudo M., Hakura A., Tanimoto T., Torigoe K., Okura T., Nukada Y., Hattori K., Akita K., Namba M., Tanabe F., Konishi K., Fukuda S. and Kurimoto M. (1995) Cloning of a new cytokine that induces IFN-γ production by T cells. *Nature* **378**, 88–91.

Parker L. C., Luheshi G. N., Rothwell N. J. and Pinteaux E. (2002) IL-1beta signalling in glial cells in wild-type and IL-1RI deficient mice. *Br. J. Pharmacol.* **136**, 312–320.

Perregaux D. and Gabel C. A. (1994) Interleukin-1β maturation and release in response to ATP and nigericin. Evidence that potassium depletion mediated by these agents is a necessary and common feature of their activity. *J. Biol. Chem.* **269**, 15195–15203.

Pinteaux E., Parker L. C., Rothwell N. J. and Luheshi G. N. (2002) Expression of interleukin-1 receptors and their role in IL-1 actions in murine microglial cells. *J. Neurochem.* **83**, 754–763.

Prinz M. and Hanisch U.K. (1999) Murine microglial cells produce and respond to interleukin-18. *J. Neurochem.* **72**, 2215–2218.

Puren A. J., Fantuzzi G., Gu Y., Su M. S. and Dinarello C. A. (1998) Interleukin-18 (IFN-γ-inducing factor) induces IL-8 and IL-1β via TNFα production from non-CD14+ human blood mononuclear cells. *J. Clin. Invest.* **101**, 711–721.

Reznikov L. L., Kim S. H., Westcott J. Y., Frishman J., Fantuzzi G., Novick D., Rubinstein M. and Dinarello C. A. (2000) IL-18 binding protein increases spontaneous and IL-1-induced prostaglandin production via inhibition of IFN-γ. *Proc. Natl Acad. Sci. USA* **97**, 2174–2179.

Rubartelli A., Cozzolino F., Talio M. and Sitia R. (1990) A novel secretory pathway for interleukin-1β, a protein lacking a signal sequence. *EMBO J.* **9**, 1503–1510.

Sanz J. M. and Di Virgilio F. (2000) Kinetics and mechanism of ATP-dependent IL-1β release from microglial cells. *J. Immunol.* **164**, 4893–4898.

Takeda K., Tsutsui H., Yoshimoto T., Adachi O., Yoshida N., Kishimoto T., Okamura H., Nakanishi K. and Akira S. (1998) Defective NK cell activity and Th1 response in IL-18-deficient mice. *Immunity* **8**, 383–390.

Wheeler R. D., Culhane A. C., Hall M. D., Pickering-Brown S., Rothwell N. J. and Luheshi G. N. (2000) Detection of the interleukin-18 family in rat brain by RT–PCR. *Brain Res. Mol. Brain Res.* **77**, 290–293.

Impaired Motor Coordination in Mice Lacking Neural Recognition Molecule NB-3 of the Contactin/ F3 Subgroup

Yasuo Takeda,[1] Keiko Akasaka,[1,3] Suni Lee,[1,4] Satoru Kobayashi,[1] Hitoshi Kawano,[5] Shigeo Murayama,[2] Naoki Takahashi,[3] Kouichi Hashimoto,[6] Masanobu Kano,[6] Masahide Asano,[7] Katsuko Sudo,[8] Yoichiro Iwakura,[8] Kazutada Watanabe[1,9]

[1] Department of Cell Recognition, Tokyo Metropolitan Institute of Gerontology, Sakaecho, Itabashi-ku, Tokyo 173-0015, Japan

[2] Department of Neuropathology, Tokyo Metropolitan Institute of Gerontology, Sakaecho, Itabashi-ku, Tokyo 173-0015, Japan

[3] Department of Metabolic Regulation in Animal Cells, Nara Institute of Science and Technology, Takayama, Ikoma, Nara 630-0101, Japan

[4] Department of Applied Biological Science, Tokyo University of Agriculture and Technology, Saiwaicho, Fuchu, Tokyo 183-8509, Japan

[5] Department of Anatomy and Embryology, Tokyo Metropolitan Institute for Neuroscience, Musashidai, Fuchu, Tokyo 183-8526, Japan

[6] Department of Physiology, Kanazawa University School of Medicine, Takaramachi Kanazawa 920-8640, Japan

[7] Institute for Experimental Animals, Kanazawa University School of Medicine, Takaramachi Kanazawa 920-8640, Japan

[8] Center for Experimental Medicine, Institute of Medical Science, University of Tokyo, Minato-ku, Tokyo 108-8639, Japan

[9] Department of BioEngineeing, Nagaoka University of Technology, Nagaoka, Niigata 940-2188, Japan

Received 31 October 2002; accepted 29 January 2003

The first two authors contributed equally to this work.

Correspondence to: K. Watanabe (kazutada@vos.nagaokaut.ac.jp).

Contract grant sponsor: Grants-in-Aid for Scientific Research from the Ministry of Education, Science, Sports and Culture of Japan.

DOI 10.1002/neu.10222

ABSTRACT: **The neural recognition molecule NB-3, which belongs to the contactin subgroup of the immunoglobulin superfamily, is expressed exclusively in the nervous system and mainly upregulated at the early postnatal stage during mouse brain development. The expression of NB-3 in the cerebellum increases until adulthood. In contrast, the expression in the cerebrum declines to a low level after postnatal day 7. To characterize the functional roles of NB-3 *in vivo*, we generated NB-3-deficient mice by substituting a part of the NB-3 gene with the β-galactosidase (Lac Z) gene. Complete overlap of the Lac Z expression in the heterozygous mouse brain with the NB-3 immunostaining pattern in the rat cerebellum and with the previously reported pattern of *in situ* hybridization of NB-3 transcripts indicated that Lac Z expression reflects the expression of NB-3 in the mouse brain. NB-3-deficient mice were viable and fertile. The formation and organization of all nuclei and layers throughout the brains of mutant mice appeared normal. Behavioral tests to examine motor function showed that the mice deficient for NB-3 were slow to learn to stay on the rotating rod in the rotorod test during repeated trials, and that they displayed dysfunction of equilibrium and vestibular senses in the wire hang and horizontal rod-walking tests. In contrast, the mutant mice showed no difference of grasp force from the wild-type mice. Thus, NB-3-deficient mice are impaired in motor coordination.**
J Neurobiol 56: 252–265, 2003

Keywords: **NB-3; immunoglobulin superfamily; knockout; cerebellum; motor coordination**

INTRODUCTION

Neural recognition molecules of the immunoglobulin (Ig)-superfamily play important roles not only in the formation of axon trajectories and synaptic connections during development, but also in synaptic plasticity and memory in adulthood (Doherty et al., 1995; Murase and Schuman, 1999). ApCAM (NCAM-related adhesion molecule in *Aplysia*) is modulated with long-term synaptic plasticity (Mayford et al., 1992). A highly polysialylated NCAM is mobilized to the cell surface of neurons in an activity-dependent manner (Kiss et al., 1994) and is required for morphological plasticity of neurons and glial cells (Theodosis et al., 1999). The expression of L1 is regulated by specific patterns of neural impulses (Itoh et al., 1995). Class I MHC gene expression is also regulated by neural activities in both the developing and mature central nervous system (Corriveau et al., 1998). Together with cellular and biochemical analyses, gene-targeted mice have been a powerful tool for demonstrating that Ig-superfamily members are involved in brain functions including synaptic plasticity, learning, and memory. NCAM-deficient mice display defects of spatial learning and hippocampal long-term potentiation (Cremer et al., 1994). L1-gene mutant mice are also defective in spatial learning (Murase and Schuman, 1999). Mice lacking Thy-1, which is highly expressed in neurons after the completion of neuronal network formation, fail to use socially transmitted cues to direct their choice of food (Mayeux-Portas et al., 2000). Thus, members of the Ig-superfamily play important roles in the higher order function in the adult brain mediated by synaptic remodeling regulated by neuronal activity.

Neural recognition molecules composed of six Ig-like and four fibronectin type III (FN III)-like domains followed by a glycosylphosphatidyl inositol (GPI) moiety at the COOH terminal are classified in the contactin subgroup of the Ig-superfamily. At present, six proteins: contactin (also known as F3 or F11), TAG-1, BIG-1, BIG-2, NB-2, and NB-3, which share 40–60% identity to each other at the amino acid sequence level, are known in this subgroup (Ogawa et al., 1996). Expression of all the subgroup members except TAG-1 is upregulated during the postnatal development of the nervous system. Mice with ablated contactin gene expression display neurological defects, including severe ataxia and hyperactivity, and survive only until postnatal day 18 (Berglund et al., 1999). Detailed analysis of the mice has further revealed that contactin is a selective neuronal component of the paranode that regulates junctional attachment between axon and glial membranes, and is indispensable for organizing the paranodal region of myelinated fibers (Boyle et al., 2001). In accordance with this, mice deficient for caspr, which functions together with contactin in a *cis* fashion, also exhibit malformation and dysfunction of the paranodal region (Bhat et al., 2001). Thus, analysis of gene-deficient mice has played an essential role in elucidation of the biological significance of contactin. We consider that generation of gene-targeted mice will also be indispensable for studying the function of other members in the subgroup whose functions have remained elusive. Especially, the generation and behavioral analysis of gene-ablated mice should be of particular use for studying proteins expressed postnatally.

We have previously reported that the expression of NB-3 transcripts in the mouse brain becomes evident after birth when overall brain architecture has been established (Lee et al., 2000). The brain regions highly expressing NB-3 transcripts are the accessory olfactory bulb, anterodorsal thalamic nuclei, inferior

colliculi, cerebral cortex, and cerebellum. Among these regions, the cerebellum has a unique pattern of expression of NB-3: the expression increases through adulthood after the completion of cerebellar development, whereas the level in the cerebrum is maximal at postnatal day 7 and declines to a low level thereafter. Based on this expression pattern, in this study, we focused our attention on the cerebellar function of NB-3 in adulthood, and we report here the generation of NB-3 knockout mice and their defects in motor coordination.

MATERIALS AND METHODS

Phosphatidyl Inositol-Specific Phospholipase C (PI-PLC) Treatment

PI-PLC treatment was performed as described previously (Ogawa et al., 2001). Briefly, rat brains at postnatal day 6 (P6) were homogenized in 1 m*M* $NaHCO_3$, pH 7.9, 0.2 m*M* $CaCl_2$, 0.2 m*M* $MgCl_2$, and 1 m*M* spermidine containing the protease inhibitors leupeptin (4.8 μg/mL), pepstatin (0.7 μg/mL), *p*-amidinophenylmethylsulfonyl fluoride hydrochloride (174 μg/mL), and aprotinin (6 μg/mL). After removal of cell debris by centrifugation at 1200 rpm for 20 min at 4°C, the homogenate was centrifuged at 14,500 rpm for 20 min at 4°C. The pellet was suspended at 0.1 μg/mL of protein in 10 m*M* Tris-HCl, pH 7.5, 150 m*M* NaCl containing the protease inhibitors listed above and incubated with 100 mU of PI-PLC (Sigma Aldlich Japan K.K., Tokyo) at 37°C for 40 min. As a negative control, reaction mixtures without the enzyme were treated in the same manner. After the reaction, samples were centrifuged at 15,000 rpm for 20 min at 4°C and subjected to Western blot analysis.

Preparation of Recombinant NB-3.His Protein

To make a construct expressing a soluble form of NB-3 protein, the signal sequence for the GPI anchor was removed from the rat NB-3 cDNA, and substituted with a sequence encoding six histidine residues with a stop codon. The cDNA thus obtained was inserted in the pREP4 expression vector (Invitrogen), and the resultant construct was transfected into 293 cells using Lipofectamine PLUS (Life Technologies Inc., Rockville, MD). The NB-3.His recombinant protein was purified from the culture medium, using Ni-NTA agarose (Qiagen) and dialyzed against phosphate-buffered saline (PBS) before use.

Primary Culture of Neuronal Cells for Measurement of Neurite Outgrowth-Promoting Activity

Cortices from Wistar rat embryos at embryonic day 16 (E16) were dissected and dispersed in Hank's balanced medium (Life Technologies Inc.). The cells were washed twice with the same medium and then suspended in Neurobasal medium containing 2% B-27 supplement (Life Technologies Inc.), 0.5 m*M* L-glutamine, and 25 μ*M* glutamate. To measure the neurite outgrowth-promoting activity, the cells were plated at 3×10^4 cells on 35-mm culture plates coated with NB-3.His and incubated for 24 h at 37°C in a CO_2 incubator. As positive and negative controls, the culture plates were coated with laminin and bovine serum albumin (BSA), respectively, instead of NB-3.His. The activity of the soluble form of NB-3 was also measured using neurons on poly-L-lysine-coated plates in medium containing various concentrations of NB-3.

Construction of Targeting Vector

The 8.4-kb fragment of genomic DNA containing exon 2 of the NB-3 gene previously isolated from a 129/SVJ mouse genomic library (Stratagene, La Jolla, CA) (Lee et al., 2000) was used to construct the gene-targeting vector. Exon 2 contains 85 bp of 5′-untranslated region and 55 bp of coding region encoding 18 amino acid residues starting from the translation initiation codon ATG (Fig. 3). In the gene-targeting vector, a 1-kb fragment from the initiation codon in exon 2 to a *Bgl* I site in intron 2 was deleted and replaced with the bacterial β-galactosidase (Lac Z) and PGK-neo-resistance genes. A diphtheria toxin A (DT) gene was added to the 3′-end of this DNA fragment as a negative selection marker. The final construct contained a 2.1-kb 5′-homologous region and a 5.3-kb 3′-homologous region.

Generation of NB-3 Knockout Mice

The linearized targeting vector was electroporated into 129/SVJ embryonic stem (ES) cells. Five hundred eighty-eight clones resistant to G418 were analyzed by nested PCR. The first PCR was performed by using the pair of primers 5′-CCTGAAAATGTAAATGCACCCTATATGC-3′ in intron 1 and 5′-ATCATCATTAAAGCGAGTGGCAACATGG-3′ in the Lac Z gene. The second PCR was performed by using the nested pair of primers 5′-CCCTCTCACAGGGCCTCCTCCCTAC-3′ and 5′-GCTGATTTGTGTAGTCGGTTTATGC-3′. Only the mutant allele generated a 3.1-kb DNA fragment. Nine clones shown to be positive by PCR were further analyzed by Southern blotting to examine whether proper homologous recombination had occurred. DNA fragments flanking the targeting vector were used as probes, as shown in Figure 3. Genomic DNA was digested with *Pst* I for analysis with the upstream probe and with *Eco* RV for analysis with the downstream probe. Using the upstream probe, the wild-type and mutant alleles gave 6- and 7-kb bands, respectively. Using the downstream probe, the wild-type allele gave a 16-kb band, while the mutant allele gave a 10.4-kb band. Finally, eight of 588 clones were found to be properly targeted. Chimeric mice were produced by an aggregation method according to the procedure described by Horai et al. (2000). Ten to 15 ES cells were aggregated with two C57BL/6 eight-cell stage embryos in a hole on a plastic dish and cultured over-

night, and well-formed blastocysts were transferred into the uterus of pseudopregnant female mice. Male chimeric mice were then bred with C57BL/6 female mice, and germline transmission was checked by monitoring the agouti coat color. Mice heterozygous for NB-3 mutation were intercrossed to yield homozygous mutants. Genotyping of the mice was performed either by Southern blotting as described above or by genomic PCR using the primers 5′-CCTTCAGATAGATTGCTAAC-3′ and 5′-AGGTTACTCTTACAACATCAC-3′ for the wild-type allele, and 5′-TAAATGTGAGCGAGTAACAAC-3′ for the LacZ gene.

Colorimetric Detection of Lac Z Expression

Mice at postnatal day 7 were perfused with PBS under pentobarbital anesthesia, and then with 2% paraformaldehyde dissolved in PIPES, pH 6.9, containing 2 m*M* $MgCl_2$, 5 m*M* EGTA. Brains were removed and postfixed overnight at 4°C. Then the brains were cryoprotected by incubation overnight in 20% sucrose containing 2 m*M* $MgCl_2$. Floating sections (50 μm) were prepared using a sliding microtome. Sections were washed twice in PBS containing 2 m*M* $MgCl_2$ and then incubated in PBS containing 2 m*M* $MgCl_2$, 0.005% sodium deoxycholate and 0.01% NP-40 for 10 min at 4°C. Colorimetric reaction was performed in the same solution containing 5 m*M* $K_3[Fe(CN)_6]$, 5 m*M* $K_4[Fe(CN)_6]$, and 0.05% 5-bromo-4-chloro-3-indolyl-β-D-galactoside (X-gal) at 37°C overnight. The sections were washed, mounted, air dried, and were counterstained with 0.5% neutral red to visualize the brain architecture.

Production of Anti-NB-3 Antibodies

We prepared two kinds of anti-NB-3 antibodies. A polyclonal rabbit antiserum that recognizes the region between the first and second Ig domains (amino acid positions 30–227) of rat NB-3 was generated by using a cDNA fragment corresponding to this region amplified by PCR with the pair of primers 5′-TCCGGATCCCATGGAGCCACAGGATGTCATTTT-3′ and 5′-TCCGGATCCGTCGACTGGCACATATTCCCCCATGA-3′. To generate a polyclonal antiserum against the second and third FN III-like domains (amino acid positions 691–879) of mouse NB-3, the primers for PCR were 5′-CATATGGAGCTGCTGAGAACCAAAGC-3′ and 5′-AGATCTACAGAGGCAAAGTAAATCGT-3′. Each amplified fragment was cloned between the *BamH* I sites or between the *Nde* I and *BamH* I sites of the pET15b bacterial expression vector and the nucleotide sequence was confirmed. Each recombinant protein tagged with six histidine residues was produced in *E. coli* BL21(DE3)pLysS and purified using Ni-NTA resin in the presence of urea followed by preparative SDS-polyacrylamide gel electrophoresis. The purified recombinant proteins were used to immunize rabbits or mice every 2 weeks. The antibody used for Western blot analysis was affinity-purified using the recombinant protein immobilized on nitrocellulose membranes.

Immunohistological Analysis

Rats and mice were perfused with PBS under pentobarbital anesthesia, and then fixed with 95% ethanol containing 5% acetic acid. Brains were removed and preserved overnight in the fixative at 4°C. The brains were embedded in paraffin and cut on a rotary microtome at 5-μm thickness. Sections were transferred onto glass slides coated with egg albumin and dried at 44°C overnight. After deparaffinization, sections were subjected to immunohistochemical analysis. Some sections were stained with 1% cresyl violet for histological examination. For immunohistochemistry of NB-3 and calbindin D-28k, sections were rehydrated through xylene and a descending ethanol series and then sequentially incubated with rabbit polyclonal antiserum against rat NB-3 antiserum (1:1000) or calbindin D-28k (1:5000; Swant Antibodies, Bellinzona, Switzerland) overnight at 4°C and peroxidase-labeled antirabbit IgG Fab′ fragment (1:100; Medical and Biological Laboratories, Nagoya, Japan). The immunoreaction was then visualized by incubation of the sections in 50 m*M* Tris buffer (pH 7.4) containing 0.01% diaminobenzidine tetrahydrochloride and 0.01% hydrogen peroxide for 5–15 min at 37°C.

Behavioral Analysis

Mice used for behavioral tests were produced by intercrossing of heterozygous mutants in a mixed background of 129/SVJ and C57BL/6. Wild-type littermates were used as a control. Behavioral tests were performed on male mice at the age of between 6 and 10 months of age. Mice were divided into three groups depending on their birth date. Each group consisted of 10–11 each of wild-type and homozygous mutant mice. In the wire-hang test, an L-shaped wire consisting of a horizontally positioned string measuring 15 cm in length and 1.5 mm in diameter flanked by two side bars of equal diameter was used. The wire was placed 30 cm above the floor. The mice were required to grasp the middle part of the horizontal string with their forepaws (Dean et al., 1981). Traction was estimated by the ability to bring at least one hindpaw up to the wire within 5 s. The time to falloff, with a 30-s cutoff time, was measured to evaluate the prehensile reflex. Three trials were performed for each mouse with a 20-min interval. The muscle strength of forepaws was measured by using a DFIS 2 digital force gauge (Chatillon, North Carolina). Mice that grasped the grid of the apparatus by their forepaws were pulled backward by their tails until they released the grid. The mean values of three trials per mouse were calculated. An inverted grid test was performed to further evaluate the neuromuscular strength of the four paws. Mice were placed on a wire grid (5-mm squares constructed with wires 1 mm in diameter) so that they would grip the wire by all four paws. The grid was then turned upside down, and placed horizontally 30 cm above the surface of soft bedding sponges. The time to fall onto the bedding was recorded, with a 300-s cutoff time. The rotorod test was performed as described previously (Storm et al., 1998; Ferguson et al., 2000). The

rotorod apparatus consisted of a ridged plastic rod (3.5-cm diameter, 30 cm long) divided into five sections by plastic circular plates (26 cm diameter) placed every 5.7 cm to separate the mice from each other. The height from the top of the rod to the platform was 16.5 cm, to prevent the mice from escaping. Mice were placed on the rotating rod at constant velocity (10 rpm) with the heading in the direction of rotation and forced to walk. The mice were allowed to stay on the rod for up to 5 min until they fell off the rod. Mice were subjected to four trials a day at 15-min intervals for 10 consecutive days. For the horizontal rod test, mice were placed on the midpoint of a stationary 68-cm horizontal wooden rod (18 mm in diameter) with platforms (12 × 14 cm) at both ends, positioned 50 cm above the floor. The number of mice that could reach the platform at either end by walking without falling off in 5 min was recorded (Dean et al., 1981). Each mouse was subjected to three trials. Behavioral scores were subjected to either single-factor ANOVA or two-way ANOVA with SAS/STAT software version 6 for Windows (SAS Inst. Inc., Cary, NC).

Electrophysiological Analysis

Sagittal cerebellar slices of 250-μm thickness were prepared from the wild-type, and mutant mice as described previously (Edwards et al., 1989; Llano et al., 1991; Kano et al., 1992; Aiba et al., 1994). A whole-cell recording was made from visually identified Purkinje cells using a 40× water immersion objective attached to an Olympus (BX50WI) upright microscope (Edwards et al., 1989; Llano et al., 1991). The resistance of patch pipettes was 3–6 MΩ when they were filled with an intracellular solution containing 60 m*M* CsCl, 10 m*M* D-glucose, 20 m*M* tetraethylammonium (TEA)-Cl, 20 m*M* BAPTA, 4 m*M* $MgCl_2$, 4 m*M* ATP and 30 m*M* HEPES, pH 7.3, adjusted with CsOH. The composition of the standard bath solution was 125 m*M* NaCl, 2.5 m*M* KCl, 2 m*M* $CaCl_2$, 1 m*M* $MgSO_4$, 1.25 m*M* NaH_2PO_4, 26 m*M* $NaHCO_3$, and 20 m*M* glucose; the solution was bubbled with a mixture of 95% O_2 and 5% CO_2. Bicuculline (10 μM) was always added to the saline to block spontaneous inhibitory postsynaptic currents (Kano et al., 1992). Ionic currents were recorded with an Axopatch-1D (Axon Instruments, Foster City, CA). Stimulation and online data acquisition were performed using PULSE software (version 8.1; HEKA Elektonik) and a Macintosh computer. The signals were filtered at 3 kHz and digitized at 20 kHz. Fitting of the decay phase of excitatory postsynaptic currents (EPSCs) was performed with PULSE-FIT software (version 8.1; HEKA Elektonik). For stimulation of climbing fibers (CFs) and parallel fibers (PFs), we used a glass pipette with a 5–10-μm tip diameter filled with standard saline. Square pulses (duration, 0.1 ms; amplitude, 0–100 V for stimulation of CFs, 1–10 V for stimulation of PFs) were applied for focal stimulation.

RESULTS

Release of NB-3 from the Cell Membrane by PI-PLC, and Neurite Outgrowth-Promoting Activity of NB-3

We treated the membrane fraction of the rat brain with PI-PLC to examine whether NB-3 is a GPI-anchored protein or not [Fig. 1(A)]. After the PI-PLC treatment, NB-3 protein was mostly observed in the supernatant whereas a negligible amount of NB-3 was detected in the membrane fraction. Without PI-PLC, the amount of NB-3 protein released from the membrane fraction was negligible. These results indicate that NB-3 is bound to the surface of the cell membrane by the GPI-moiety.

To evaluate the neurite outgrowth-promoting activity of NB-3, neuronal cells derived from the cerebral cortex of Wistar rat brains at E16 were plated on dishes coated with NB-3.His protein. The cortical neurons extended longer neurites on the NB-3 substrate than on BSA [Fig. 1(B)]. The average length of the neurites on the NB-3 substrate was approximately two-thirds of that on laminin. Cortical neurons that were cultured on poly-L-lysine in medium containing the soluble form of NB-3 also exhibited longer neurites in a manner dependent on the dose of NB-3 [Fig. 1(C)]. Thus, both the substrate-bound and the soluble form of NB-3 protein had a neurite outgrowth-promoting effect on cortical neurons.

Localization of NB-3 in the Rat Cerebellum

Our previous studies demonstrated that NB-3 transcripts were expressed in the developing mouse cerebellum at P1 and P7 (Lee et al., 2000). Here, we examined the localization of NB-3 protein in the cerebellum of 3-month-old rats using anti-rat NB-3 antiserum (Fig. 2). The granule cells and the molecular cell layer exhibited intense NB-3 immunoreactivity in lobules 1–8, whereas the immunoreactivity was weak in the molecular layer of lobules 9 and 10. Interestingly, comparison of two consecutive sections, one stained by Nissl staining and the other immunostained for NB-3, demonstrated that only subpopulations of the granule cells exhibited NB-3 immunoreactivity. On the other hand, the Purkinje cells did not exhibit NB-3 immunoreactivity in lobules 1–8, while the dendrites and somata of the Purkinje cells in lobules 9 and 10 did exhibit NB-3 immunoreactivity. Thus, the NB-3 immunostaining pattern in lobules 1–8 was distinct from that in lobules 9 and 10.

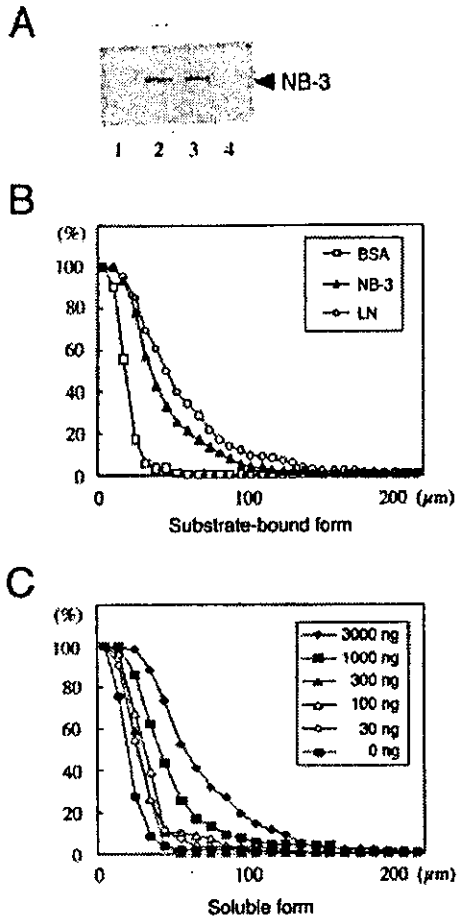

Figure 1 Release of NB-3 protein from the membrane by PI-PLC treatment, and neurite outgrowth-promoting activity of NB-3. (A) The crude membrane fraction and supernatant were subjected to SDS-PAGE, followed by Western blot analysis using anti-NB-3 antiserum. In lanes 1 and 2, the membrane fraction and supernatant after separation of PI-PLC-treated lysate were applied, respectively. Lanes 3 and 4 show the control membrane fraction and supernatant derived from lysate not treated with PI-PLC, respectively. (B) Cortical neurons from rat cerebrum at E16 were plated on NB-3, laminin, or BSA as substrate. (C) The neurons were cultured on poly-L-lysine in the presence of various amounts of the soluble form of NB-3. In (B) and (C), the percentage of neurons (ordinate) with neurites longer than the diameter of the soma in micrometers (abscissa) is plotted. Two hundred to 800 neurons were counted for each condition. LN, laminin.

Generation of NB-3 Knockout Mice by Homologous Recombination

NB-3 mutant mice were generated by homologous recombination in embryonic stem cells. We replaced the genomic region of NB-3 encoding the secretion signal and a part of the first Ig-domain with LacZ and Neo genes [Fig. 3(A)]. Because the Lac Z gene was placed just downstream of the ATG initiation codon, the mutant mice were expected to produce Lac Z protein instead of NB-3 protein. Genotypes were determined by Southern blot or PCR analyses. The genomic DNAs digested with *Pst* I gave a 6-kb band for the wild-type and a 7-kb band for the mutated alleles, respectively, when probed with probe A [Fig. 3(B)]. When probe B was used to probe the genomic DNAs digested with *Eco* RV, 16- and 10.4-kb bands were detected for the wild-type and mutant alleles, respectively (data not shown). Probe C was used to confirm that there was a single copy of the Neo gene in the genome. Genotyping of the mice was also performed by genomic PCR, which gives 263- and 501-bp bands for the wild-type and mutant alleles, respectively [Fig. 3(C)].

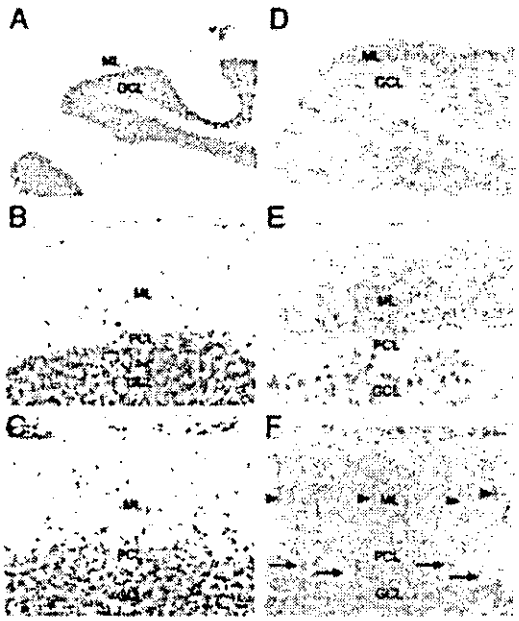

Figure 2 Localization of NB-3 protein in the cerebellum of a 3-month-old rat. (A, D) Lobule 2 at low magnification. (B, E) Lobule 2 at high magnification. (C, F) Lobule 9 at high magnification. (A–C) Nissl staining. (D–F) NB-3 immunostaining. Arrowheads and arrows indicate the dendrites and somata of the Purkinje cells, respectively. Note that NB-3 protein is localized in the molecular layer and subpopulations of the granule cells, but not in the Purkinje cells in lobule 2, whereas the dendrites and somata of the Purkinje cells in lobule 9 exhibit NB-3 immunostaining, but there is little immunostaining in the molecular layer. GCL, granule cell layer; ML, molecular layer; PCL, Purkinje cell layer.

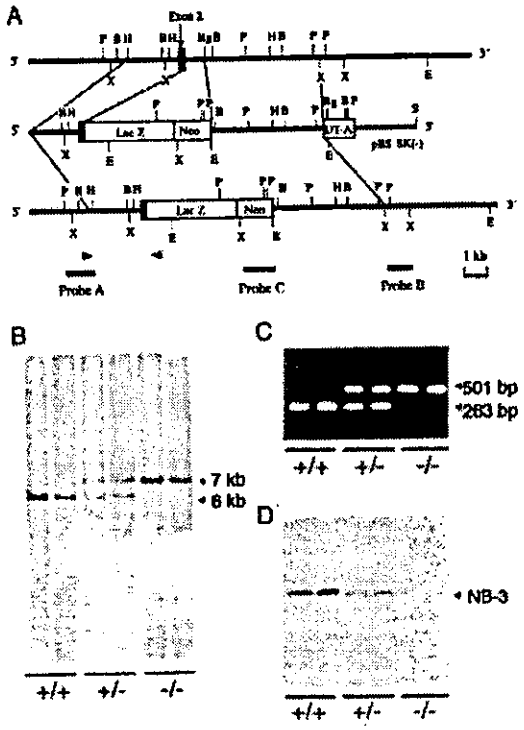

Figure 3 Targeted disruption of the gene encoding NB-3. (A) Schematic representation of the wild-type allele (top), the targeting vector (middle), and the predicted mutant allele (bottom). The second exon is indicated by a filled box and encodes a 5′-untranslated sequence and the first 17 amino acids of a signal peptide. The targeting vector contained a PGK-neo cassette and a DT cassette. Arrowheads represent the approximate positions of primers for PCR. Probes A, B, and C, indicated by hatched lines, were used for detection of homologous recombination of the NB-3 gene with the targeting vector by Southern blot analysis. B, *BamH* I; Bg, *Bgl* II; E, *Eco* RV; H, *Hind* III; P, *Pst* I; S, *Sac* II; X, *Xba* I (B) Southern blot analysis for verification of genotypes. Genomic DNAs were digested with *Pst* I and hybridized with probe A. The 6- and 7-kb bands were derived from wild-type and mutant alleles, respectively. (C) Allele-specific PCR analysis performed with genomic DNAs isolated from the tails of the offspring (F2) of the heterozygous crosses. The 501-bp band was generated only from the mutant allele (top), whereas the 263-bp band was generated from the wild-type allele (bottom). (D) Western blot analysis of brain extracts from the NB-3 (+/+), (+/−) and (−/−) mice with anti-NB-3 antiserum. Mouse whole brains were homogenized in SDS sample buffer and 10 μL of the homogenate was applied to each well.

We next examined whether homozygous mice were deficient for NB-3 protein or not by using two kinds of anti-NB-3 antibodies (described in Materials and Methods) that recognize different regions not including the region encoded in the gene region deleted in the knockout mice. NB-3 protein was not detected in the homozygous mice by Western blot analysis using these antibodies [Fig. 3(D)]. As expected, NB-3 protein levels in the heterozygous mice were approximately 50% of those found in the wild-type mice.

Expression Patterns of NB-3 Monitored by X-gal Staining in Heterozygotes

We expected that in the mutant mice, expression of the inserted Lac Z gene would be driven by the promoter of the NB-3 gene. The expression of Lac Z was visualized by X-gal staining, which showed a strong blue color in the accessory olfactory bulb, anterodorsal thalamic nuclei, inferior colliculi, and layer 5 of the cerebral cortex, in addition to the cerebellum (Fig. 4). The staining pattern was essentially the same as that observed by *in situ* hybridization for NB-3 and previously reported by our group (Lee et al., 2000). Thus, the Lac Z gene expression

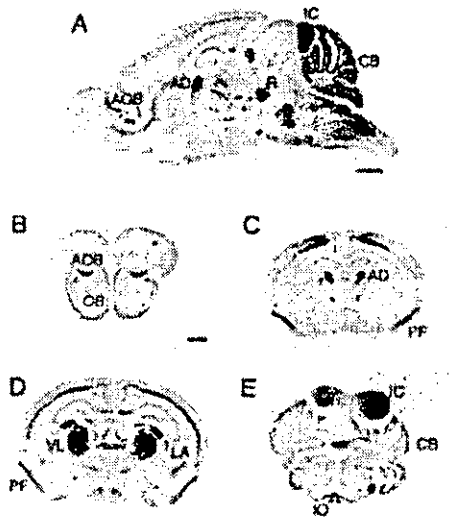

Figure 4 The localization of the cells expressing NB-3 monitored by Lac Z expression. Brain sections from 14-day-old NB-3 (+/−) mice were stained with X-gal. The blue color represents Lac Z gene expression, which reflects the cells expressing the NB-3 gene. The sections were then counterstained with 0.5% neutral red. In (A), a sagittal section is shown. Coronal sections from heterozygotes are displayed in (B–E). Scale bars indicate 1 mm. AOB, accessory olfactory bulb; AD, anterodorsal thalamic nucleus; CB, cerebellum; IC, inferior colliculus; IO, inferior olive; LA, lateral amygdaloid nucleus; OB, olfactory bulb; PF, piriform cortex; R, red nucleus; VL, ventrolateral thalamic nucleus.

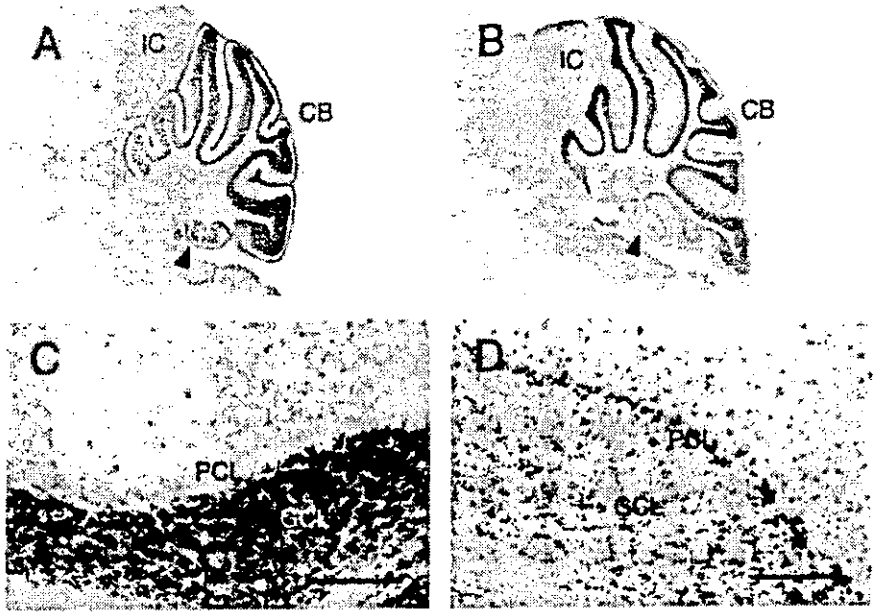

Figure 5 Developmental expression pattern of NB-3 monitored by Lac Z expression in the cerebellum. Blue color represents expression of the Lac Z gene. The sections were counterstained with 0.5% neutral red. Sagittal sections from heterozygous mice at P14 (A) and 6 months of age (B) are shown. (C, D) High-magnification views of lobules 8 and 10 of the 6-month-old cerebellum. Arrowheads indicate lobule 10. NB-3 was expressed only in the Purkinje cell layer of lobule 10 at P14. Lobules 1 to 8 expressed NB-3 strongly in the granule cells in the 6-month-old mouse cerebellum, whereas there was little if any NB-3 expression in the Purkinje cells in these lobules. Scale bars indicate 100 μm. CB, cerebellum; IC, inferior colliculus; GCL, granule cell layer; PCL, Purkinje cell layer.

was controlled by the promoter of the NB-3 gene in the mutant mice, and accordingly reflected the expression of NB-3.

The developmental expression of NB-3 in the cerebellum exhibited dynamic changes. In the cerebellum at postnatal day 7, the Purkinje cells in lobule 10 were strongly stained with X-gal (Fig. 5). In adulthood, the staining in the Purkinje cells was intense in lobule 10 and the caudal half of lobule 9, and was weak in other lobules. On the other hand, the staining in the internal granule cells gradually became evident in all lobules except lobule 10 and the caudal half of lobule 9 as the mice approached adulthood. Finally, the granule cells were densely stained with X-gal in 6-month-old mice. The granule cells in lobule 10 and the caudal half of lobule 9 were slightly stained. This indicates that NB-3 is highly expressed in the internal granule cells in lobule 1 to the rostral half of lobule 9, but only in part of the Purkinje cells in the adult mouse cerebellum. Thus, the expression of NB-3 showed a distinct difference between the rostral and caudal lobules, with a boundary in lobule 9.

Normal Appearance and Normal Brain Architecture in NB-3 Knockout Mice

NB-3 knockout mice were viable, fertile, and largely indistinguishable from their wild-type littermates. The gender and genotype ratios of offspring born from NB-3 heterozygous intercrosses conformed to the expected Mendelian frequency. No difference was observed in general appearance or overt behavior between the wild-type and knockout mice. The body weight and overall brain sizes of NB-3 (−/−) mice also appeared normal.

The organization of the cerebrum of the NB-3 (−/−) mice was indistinguishable from that of the NB-3 (+/+) mice by staining with not only Nissl staining (Fig. 6) but also with antibody against neurofilaments (data not shown). Likewise, the cerebellum of the NB-3 (−/−) mice exhibited well-developed foliation, comparable to that of the NB-3 (+/+) mice. Laminar structure in the cerebellar cortex where the Purkinje cells were aligned in a monolayer between the granular cell and molecular layers was clearly discernible in the mutant mice by the staining

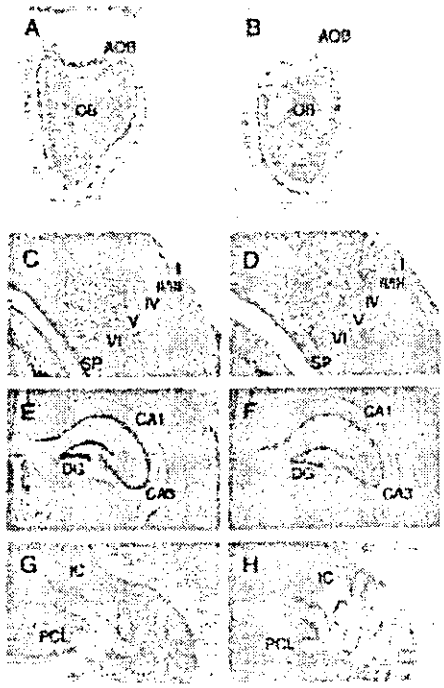

Figure 6 Brain organization of the NB-3 knockout mice. The brain sections from various parts of the NB-3 (+/+) (A, C, E, and G) and (−/−) mice (B, D, F, and H) at P7 were stained by Nissl staining (A–F) or immunostained with anti-calbindin antibody (G–H). (A, B) Olfactory bulb; (C, D), cerebral cortex; (E, F) hippocampus; (G, H) cerebellum. AOB, accessory olfactory bulb; DG, dentate gyrus of the hippocampus; OB, olfactory bulb; PCL, Purkinje cell layer; I–VI, layers I–VI of the cerebral cortex; SP, subplate.

with antibody against calbindin. Thus, the cytoarchitecture of the brain is not significantly different between the NB-3 (+/+) and (−/−) mice at the light-microscopic level. Ultrastructural analysis of the molecular layer of lobule 10 by electron microscopy also showed well-developed Purkinje cell dendrites and PFs in the knockouts (data not shown).

NB-3 Knockout Mice Show Defects in Motor Coordination

Monitoring of NB-3 expression by X-gal staining in NB-3 (+/−) mice together with our previous results (Lee et al., 2000) showed a high level of expression in the adult cerebellum, suggesting a possible role of NB-3 in motor function. Therefore, we analyzed the motor abilities of the NB-3 (−/−) adult mice in detail. We tested 28 mice with each genotype obtained from heterozygous intercrosses. The NB-3 (+/+) and (−/−) mice used for the behavioral tests had 34.7 ± 3.2 g and 33.3 ± 2.5 g average body weight, respectively. Mice weighing less than 30 g or more than 40 g were not used for the tests.

First, psychomotor coordination and the integrity of the vestibular system were evaluated by testing the ability of the mice to traverse a stationary horizontal rod. In three trials of the rod walking test, 17 out of 28 NB-3 (−/−) mice never reached the platform at the end of the rod. In contrast, eight out of 28 NB-3 (+/+) mice could not reach the platform in the three trials. The horizontal rod was traversed by an average of 9.3 ± 0.5 NB-3 (−/−) mice and 15.7 ± 0.9 NB-3 (+/+) mice (Table 1), indicating a significant difference in rod walking between the two genotypes ($\chi^2 = 5.85$, $p < 0.05$).

Second, a test for traction was performed by applying the wire-hang test to estimate the motor function directly. The traction reflects the equilibrium, muscle strength and tone. In the wire-hang test, mice attempt to assume a safe posture to grasp the wire by their hind paws, because of the instability of their

Table 1 Behavioral Tests for Motor Function

	NB-3 (+/+)	NB-3 (−/−)
Rod walking		
Number of mice that never reached the platform	8	17
Number of mice that reached the platform	15 ± 0.9	9.3 ± 0.5
Wire hang		
Number of mice taking a safe posture within 5s	15	2
Number of mice on the wire for 30 s	15	8
Inverted grid		
Number of mice on the grid for 30 s	18.3 ± 1.7	12.3 ± 1.2
Latency before falling (second)	64.3 ± 9.2	54.9 ± 12.2
Force gauge (gram)	89.5 ± 2.7	85.1 ± 2.7

For the rod walking and inverted grid tests, the values are shown as average values of three trials. In the wire-hanging test, mice that succeed in taking a safe posture within 5 s or staged on the were for 30 s at least once in two trials were executed as described by Dean et al.(1981).

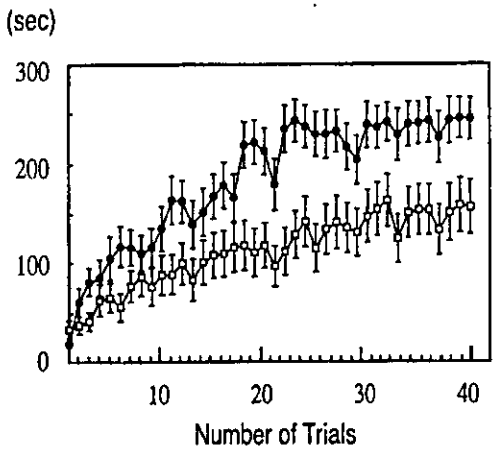

Figure 7 Performance of the NB-3 knockout mice in the rotorod test. NB-3 (+/+) (closed circles) and (−/−) (open circles) mice were placed on the rotorod, and latencies before falling from the rotorod were measured while the rod was rotating at a constant velocity of 10 rpm. Bars indicate the standard error. The results were analyzed by two-way repeated-measures ANOVA with the factors genotype, day, and trial ($p = 0.001$).

body position. Fifteen out of the 28 NB-3 (+/+) mice could bring at least one hind paw to the wire within 5 s, whereas only two out of 28 NB-3 (−/−) mice succeeded in this trial ($\chi^2 = 14.27, p < 0.001$). On the other hand, the difference in the number of mice able to hang on the wire for 30 s between the two genotypes was not significant ($\chi^2 = 3.62, p > 0.05$).

Third, we tested the performance of each genotype on a rotorod to evaluate the motor coordination of the mice objectively (Fig. 7). Both NB-3 (+/+) and (−/−) mice improved their performance with increasing trials. However, the NB-3 (+/+) mice rapidly improved their time of staying on the rotating rod with repeated trails, while the NB-3 (−/−) mice were slow to improve their time. After the 40th trial, 19 wild-type mice successfully remained on the rotorod for 300 s and three mice fell off within 30 s. In contrast, 12 NB-3 (−/−) mice could stay on the rotorod, with the trembling of their hindquarters accentuated by the effort, while 11 mice fell off within 30 s. The main effect of genotype, $F(1, 54) = 8.34, p < 0.005$, the main effect of trial, $F(39, 2106) = 26.30, p < 0.0001$, and the genotype interaction, $F(39, 2106) = 2.54, p < 0.0001$, were significant for latency before falling on the rotorod test. Thus, the wild-type mice were superior to the NB-3 knockout mice in the ability to stay and walk on the rotating rod. These results indicate that NB-3 knockout mice have poor ability to improve their sensori-motor skills upon repeated trials.

Finally, muscle strength was evaluated by testing the prehensility of the mice in the wire-hang and inverted-grid tests, and by direct measurement using a force gauge. Neither test showed any significant difference ($p > 0.05$ in Student's t test) between the NB-3 (+/+) and (−/−) mice. Thus, the muscle strength was normal in the NB-3 (−/−) mice ($p > 0.05$ in Student's t test).

Normal Excitatory Synaptic Function in the Cerebellum of the NB-3 Knockout Mice

To examine whether motor coordination defects in NB-3 knockouts result from a disorder of the synaptic transmission in the cerebellum or not, we analyzed the cerebellar synaptic function of the NB-3 (−/−) mice using electrophysiological measurements. Midsagittal cerebellar slices (250 μm) were prepared from 1.5–2-month-old mice. We first analyzed the kinetics of CF-EPSCs and PF-EPSCs. The 10–90% rise time and decay time constants were measured. The kinetics of both the rise and decay time-constants were similar in NB-3 (+/+) and (−/−) mice. Neither the amplitude nor the conductance of CF-EPSCs or PF-EPSCs was apparently changed in the NB-3 (−/−) mice (Table 2).

During early postnatal development, Purkinje cells are innervated by multiple CFs. Thereafter, synaptic elimination proceeds, resulting in the establishment of single CF innervation at the third postnatal week (Crepel, 1992). We next examined whether an abnor-

Table 2 Kinetics of CF-EPSCs and PF-EPSCs

			10–90% Rise Time (ms)	Decay Time Constant (ms)	Cord Conductance (nS)
CF-EPSC	NB3 (+/+)	($n = 17$)	0.4 ± 0.1	4.7 ± 1.2	129 ± 89
	NB3 (−/−)	($n = 11$)	0.4 ± 0.1	4.3 ± 0.6	140 ± 46
PF-EPSC	NB3 (+/+)	($n = 7$)	0.9 ± 0.2	10.1 ± 5.0	
	NB3 (−/−)	($n = 8$)	1 ± 0.2	9.1 ± 4.5	

All data are described as mean ± SD. Delay time Constants were obtained by filling the EPSC decay with a single exponential. The amplitudes of CF-EPSCs and PF-EPSCs were measured at the holding potential of −20 mV.

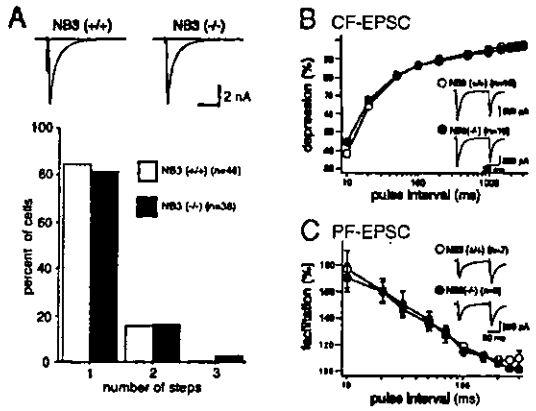

Figure 8 Electrophysiology of cerebellar synaptic functions of NB-3 knockout mice. (A) Climbing fiber innervation of Purkinje cells. Summary histograms showing number of discrete steps of CF-EPSCs of NB-3 (+/+) (open columns; n = 46) and NB-3 (−/−) (closed columns; n = 38) Purkinje cells. Data were obtained from mice at 1.5–2 months. The percentage of Purkinje cells with more than two discrete CF-EPSC steps was similar in the two genotypes ($p > 0.05$; χ^2 test for independent samples). (B) Paired-pulse depression of CF-EPSCs of the wild-type (open circles) and NB-3 knockout (closed circles) mice. The amplitude of the second response is expressed as a percentage of that of the first response (mean ± S.E.M.) and is plotted as a function of interpulse intervals. Stimulus pairs were applied at 0.1 Hz. (C) Paired-pulse facilitation of PF-mediated EPSCs. The amplitude of the second response is expressed as a percentage of that of the first response (mean ± S.E.M.) and is plotted as a function of interpulse intervals. Stimulus pairs were applied at 0.2 Hz.

mal retention of multiple CF innervation is observed in NB-3 (−/−) mice. Purkinje cells of 2-month-old NB-3 (−/−) mice showed single CF innervation [Fig. 8(A)]. Paired-pulse depression of CF-EPSCs at interpulse intervals of 10–3000 ms was not affected by lack of NB-3 [Fig. 8(B)]. Furthermore, no effect was observed on the paired-pulse facilitation of PF-EPSCs [Fig. 8(C)], suggesting that there are no significant differences in the short-term plasticity of either CF or PF synapses between NB-3 (+/+) and (−/−) mice.

DISCUSSION

To clarify the biological roles of NB-3 in brain function, we generated mice lacking NB-3 protein and performed behavioral analyses of these mice. We thereby detected a significant defect of motor coordination in NB-3 knockout mice.

Overall Brain Architecture is Normal in the Absence of NB-3

We detected no obvious abnormality in the brain organization of the mice deficient for NB-3. In the cerebrum, the overall architecture is established before birth. By contrast, the expression of NB-3 begins after birth. Accordingly, we expected the gross cerebral organization of the mutant mice to be formed normally. On the other hand, neuronal migration in the cerebellum continues after birth. In the NB-3 knockout mice as well as the wild-type mice, Purkinje cells aligned to form a single cell layer at postnatal day 7, and granule cells moved normally into the internal granule cell layer during the second to third postnatal weeks. These observations can be accounted for by the fact that a negligible amount of NB-3 is expressed in the granule cells and Purkinje cells before settlement in their final positions and elongation of their processes during early postnatal development. Thus, the spatio-temporal expression of NB-3 during development is in accord with the idea that the ablation of NB-3 expression does not impair the cell migration or process elongation steps, resulting in apparently normal brain architecture.

NB-3 Exhibits a Distinct Expression Pattern in the Cerebellum

Immunohistochemistry of the cerebellum from 3-month-old rats demonstrated that lobules 1–8 are distinct from lobules 9 and 10 with respect to the localization of NB-3 protein. In lobules 1–8, NB-3 protein was localized in the molecular layer and subpopulations of the granule cells. In these lobules, no NB-3 protein was detected in the Purkinje cells. In lobules 9 and 10, by contrast, NB-3 immunoreactivity was detected in the dendrites and somata of the Purkinje cells, and was weak in the molecular cell layer.

Lac Z gene expression in the heterozygotes visualized by X-gal staining also reflected the expression of the NB-3 gene. We examined NB-3-expressing cells in the mouse brain by evaluating X-gal staining. After formation of the overall architecture of the brain, the expression of NB-3 declined to a low level in the cerebrum. In contrast, the expression in the cerebellum displayed a unique pattern. The expression of NB-3 began in Purkinje cells of lobules 9 and 10, and was followed by expression in the internal granule cells of all lobules during cerebellar development. The NB-3 expression in the Purkinje cells was most obvious in lobules 9 and 10 in adults. Conversely, the expression in the granule cells in lobules 1 to the rostral half of lobule 9 was upregulated during

the third postnatal week and reached a maximum level at 1 month after birth. Thereafter, the expression continued at a high level in adulthood. On the other hand, the level of NB-3 expression was low in lobules 9 and 10.

Comparison of the patterns of X-gal staining and NB-3 immunostaining revealed that intense NB-3 immunostaining was detected not only in the granule cell layer, but also in the molecular layer, whereas little X-gal staining was detected in the molecular cell layer. NB-3 immunostaining in the molecular layer suggests that NB-3 is localized in axons of granule cells named parallel fibers, and is consistent with previous reports that contactin subgroup molecules are mainly localized in axons (Yoshihara et al., 1994). On the other hand, it is known that Lac Z protein fails to readily diffuse into axons (Callahan and Thomas, 1994), and thus a low level of X-gal staining (which reflects Lac Z gene expression driven by the NB-3 promoter) was observed in the molecular layer. Accordingly, the difference in the staining patterns obtained with the two different methods was due to the different characteristics of Lac Z protein and NB-3 protein. Taking this into consideration, the expression pattern of NB-3 obtained by X-gal staining was thus completely consistent with that from NB-3 immunostaining. The onset of the NB-3 expression that continues through adulthood occurs at the final stages of functional maturation during cerebellar development.

Lobules 9 and 10 are distinct from other lobules in their function. These lobules, together termed the vestibulocerebellum, project to the vestibular nucleus and are important for the control of axial and proximal limb muscles to maintain balance, the control of eye movements, and coordination of the movements of the head and eyes. The differences between the expression of NB-3 in the vestibulocerebellum versus other regions in the cerebellum may yield clues about the functional differences between these regions at the cellular level. Taken together, these facts prompted us to examine the motor functions of the adult NB-3 mutant mice.

NB-3 Is Significantly Involved in Motor Coordination

A series of behavioral tests for motor function revealed that NB-3 knockout mice showed significant defects in motor coordination, but not in muscle strength. Especially in the rotorod and horizontal rod tests, the NB-3 (−/−) mice were inferior to the wild-type mice in their ability to walk on the rods, indicating that NB-3 (−/−) mice are impaired in balance control. In this respect, it is noteworthy that the expression of NB-3 in the Purkinje cells was restricted to the vestibulocerebellum in adults. The impairment may, at least in part, originate from the lack of NB-3 in these lobules. In addition, the lack of NB-3 in granule cells in the knockouts might have accelerated the impairment. These observations suggest that the malfunction of the neuronal cells may be caused by the lack of NB-3 in adulthood.

Mice lacking contactin exhibit severe ataxia and die before postnatal day 18 (Berglund et al., 1999). Ablation of contactin gene expression affects micro-organization of the cerebellum, including orientation and fasciculation of parallel fibers, dendritic expansions of granule cells, dendritic projections of Golgi cells and axonal varicosities of the Purkinje cells. The critical role of the micro-organization of cerebellar architecture seems to be consistent with the fact that contactin was expressed throughout the postnatal stages of the cerebellar development. Studies of contactin knockout mice played an essential role in demonstrating that contactin functions in the paranodal region of the sciatic nerve to form or maintain the structure along with caspr (Bhat et al., 2001; Boyle et al., 2001). Unlike the contactin knockout mice, the NB-3 knockouts did not display ataxia in standard environments but were impaired in motor coordination when challenged. Especially, the NB-3 knockout mice were slower in learning to walk on the rotating rod than the wild-type mice, although no difference was detected between the two genotypes in latency before falling off at the beginning of the trials. Adaptation of automated compound movements to novel environments is one of the important functions of the cerebellum (Raymond et al., 1996), suggesting that this function is particularly disturbed in NB-3 knockout mice. In this context, it should be noted that the expression of NB-3 begins later than that of contactin in the developing cerebellum, indicating that these two proteins have different roles in cerebellar function.

Impaired motor coordination was previously reported in mice that lack one of the neural Ig-superfamily proteins, Punc, which contains four Ig-like and two FNIII-like domains with a transmembrane region (Yang and Mansour, 2001). Based on the particularly strong expression of the punc gene in the Bergmann glia of the cerebellum and impaired motor coordination in the Punc-knockout mice, it was suggested that Punc may play a role in the cerebellar control of motor coordination during adulthood. Like the NB-3-knockout mice in the present study, however, the mice deficient for Punc were overtly normal. Our results together with these about Punc-knockout mice suggest that subgroups in the neural Ig-superfamily might